Quaternary Research 71 (2009) 354–360

Contents lists available at ScienceDirect

Quaternary Research

journal homepage: www.elsevier.com/locate/yqres

Short Paper

Microatoll record for large century-scale sea-level fluctuations in the mid-Holocene

Ke-Fu Yu [a,b,*], Jian-Xin Zhao [b,*], Terry Done [c], Te-Gu Chen [a]

[a] South China Sea Institute of Oceanology, Chinese Academy of Sciences, Guangzhou 510301, China
[b] Radiogenic Isotope Laboratory, Center for Microscopy and Microanalysis, The University of Queensland, Qld 4072, Australia
[c] Australian Institute of Marine Sciences, Townsville, Qld 4810, Australia

ARTICLE INFO

Article history:
Received 25 March 2008

Keywords:
Microatoll
Sea level
Mid-Holocene
South China Sea
U-series
Coral reef

ABSTRACT

Coral microatolls have been long used as precise indicators of past sea level, but their use for precise definition of detailed sea-level fluctuations is still rare. Here we report twelve high-precision thermal ionization mass spectrometric ^{230}Th ages for twelve rims of five mid-Holocene microatolls from an emerged reef terrace at Leizhou Peninsula, northern South China Sea. This is a tectonically stable area, enabling us to reconstruct both the timing and trajectory of local sea-level fluctuations accurately. The elevations of these microatoll rims and cores were accurately determined relative to the surface of modern living microatolls at the same site. The results indicate that the sea level during the period of 7050–6600 yr bp (years before AD 1950) was about 171 to 219 cm above the present, with at least four cycles of fluctuations. Over this 450 yr interval, sea level fluctuated by 20–40 cm on century scales.

Introduction

Understanding the extent and timing of decadal- to century-scale sea-level fluctuations during the mid-Holocene could potentially help us to evaluate present and future changes under the influence of anthropogenic global warming. There is a strong evidence that the mid-Holocene was warmer than present (Gagan et al., 1998; Yu et al., 2005) and that relative sea level then was higher than now (Chappell, 1983; Mitrovica and Milne, 2002). But until now, little quantitative information has been known on this topic, due to the lack of a high-resolution and high-precision sea-level proxy. Living microatolls on intertidal reef flats are circular coral colonies with a flat-topped, dead core surrounded by a living rim. They have great potential as sea-level proxies, because it is prolonged subaerial exposure at low tide that kills the coral's upper surface as it grows vertically, and constrains subsequent growth to the horizontal plane (Fig. 1). Accordingly, the absolute elevation of the upper rim of live coral tissue is determined by the relative durations of submersion and subaerial exposure, which are in turn strongly linked to sea level (Habrant and Lathuiliere, 2000; Scoffin and Stoddart, 1978; Taylor et al., 1987; Woodroffe and McLean, 1990; Zachariasen et al., 1999; Zachariasen et al., 2000).

There are other causes of microatoll formation, such as excessive sedimentation (Guilcher, 1988), nutrient uptake (Steven and Atkinson, 2003) and currents (Stoddart and Scoffin, 1979). However in reef-flat settings, sea level is often the unambiguous and dominant driver of microatoll formation (Scoffin and Stoddart, 1978; Smithers and Woodroffe, 2000; Stoddart and Scoffin, 1979; Zachariasen et al., 2000). For instance, detailed analyses of 282 microatolls on 19 separate reef sites in Cocos (Keeling) Islands (Smithers and Woodroffe, 2000) show that the upper surfaces of individual microatolls were relatively horizontal and, in the case of those microatolls with their vertical growth clearly controlled by sea level alone, their mean height variation is only 2–3 cm. Because of this precise relationship between low tide level and coral rim height, the topographies of microatolls have been successfully used to detect detailed sea-level fluctuations and considered as tide gauges for the past tens to hundred years (Flora and Ely, 2003; Smithers and Woodroffe, 2001; Spencer et al., 1997; Woodroffe and McLean, 1990). However, although the emergence (above present low tide) of microatolls has been widely acknowledged as an indicator of high Holocene sea level (Chappell, 1983; McLean et al., 1978; Nott, 2003; Nunn, 2000; Nunn and Peltier, 2001; Woodroffe and McLean, 1990; Woodroffe and Gagan, 2000; Woodroffe et al., 1999), few studies have used the rims of mid-Holocene microatolls to reconstruct detailed sea-level oscillations. In this paper, we focus on detailed sea-level history by using accurate surveying of elevation and high-precision thermal ionization mass spectrometric (TIMS) U-series dating of individual rims of mid-Holocene microatolls.

Sample selection, analytical methods and results

The study was undertaken on the Leizhou Peninsula on the northern coast of the South China Sea. The emerged coral reef

* Corresponding authors. K.-F. Yu is to be contacted at South China Sea Institute of Oceanology, Chinese Academy of Sciences, Guangzhou 510301, China. Fax: +61 7 3365 8530. J.-X. Zhao, Radiogenic Isotope Laboratory, Room 214C, Richard Building, University of Queensland, Brisbane, Qld 4072, Australia. Fax: +61 7 3365 8530.
E-mail addresses: yukefu@gmail.com (K.-F. Yu), j.zhao@uq.edu.au (J.-X. Zhao).

0033-5894/$ – see front matter.
doi:10.1016/j.yqres.2009.02.003

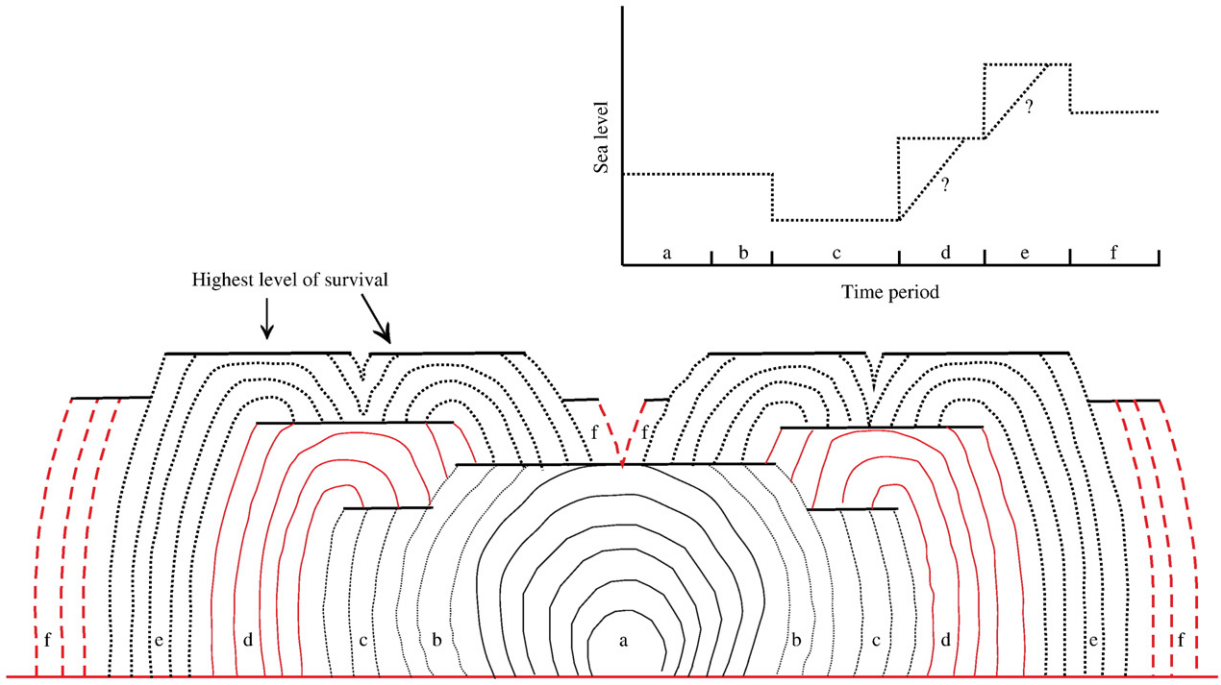

Figure 1. Relationship between microatoll developments and sea-level fluctuations. This figure shows detailed process of microatoll responses to sea-level change (after Woodroffe and McLean, 1990; Zachariasen et al., 1999). Usually, when a coral reaches the lowest tide level or the highest level of coral survival (HLS) (a), its upward growth will cease (because the coral tissue will die of exposure) but the horizontal growth will continue (b); then, as sea level drops, the HLS will also drop and coral will grow laterally at a relatively lower level (c). Later, if sea level rises again, coral will grow both upward and outward until it reaches the HLS (d); If sea level rises continuously, coral will continue the growth and even cover the old surface until it reaches the HLS (e); later, if sea level drops, coral will grow only laterally (f).

(20°13'N–20°17'N, 109°54'E–109°58'E), named Dengloujiao, 10 km long and 0.5–1.0 m wide (~2 km at the most), is a well-preserved fringing reef dominated by *Porites* and *Goniopora* species. Tectonically, the study area has been relatively stable with negligible vertical movements since the mid-Holocene (Nie et al, 1997; Lu, 1997). A historical disastrous earthquake (with magnitude M_w ~7.5) striking the neighboring Hainan Island in 1605 AD resulted in subsidence of the surrounding area (Zhang et al, 2008). However, no evidence was found to show it had any obvious impact on Leizhou Peninsula, as the two areas are separated by Qiongzhou Strait (with water depth ~100 m and width ~30 km). The tectonic stability with minimal vertical movements since mid-Holocene enables us to reconstruct both timing and trajectory of detailed local sea-level fluctuations precisely. Previous studies (Yu et al., 2002b) revealed that the coral reef formed its geomorphological framework during the mid-Holocene. Its morphology contains signatures of multiple Holocene sea-level highstands (Zhao and Yu, 2002, 2007) and also records high-frequent winter cooling and mass coral mortalities (cold-bleaching) during the Holocene climate optimum (7.5–7.0 ka) (Yu et al., 2002a; Yu et al., 2004), and a general decreasing trend in sea-surface temperature (SST) from ~6.8 to 1.5 ka with mean Sr/Ca-SSTs from 6.8 to 5.0 ka being 0.9–0.5°C higher than at present (Yu et al., 2005).

Dead microatolls, mainly *Porites* with diameters up to 9.6 m, are widespread on the emerged reef flat. Modern living *Porites* microatolls, with diameters about 0.6–1.2 m, are developing sporadically around the inner (landward) part of the modern reef flat. Thirteen samples were collected from twelve rims of five *Porites* microatolls, and their individual elevations were surveyed relative to the average elevation of the rims of modern living *Porites* microatolls, which vary within ±8.5 cm (corresponding to a maximum range of 17 cm).

The ±8.5 cm variation in elevations of the modern microatoll surfaces is similar to those observed for reef-flat microatolls at Cocos Island (from ±1.5 to ±13 cm at different sites, with a mean of ±5.5 cm) (Smithers and Woodroffe, 2001) and for microatolls near 3°S (±5 cm) (Natawidjaja et al, 2004). Smithers and Woodroffe (2001) attributed the relatively large variation in the elevations of individual microatoll colonies from different sites as mainly due to ponding as well as spatial variation in the tidal curve generated by geomorphological and hydrodynamic setting. However, they found that the mean height of living coral (HLC) within each microatoll colony shows very little variation, only 3.3±1.7 cm for the entire 282 microatolls surveyed. Based on this observation, it can be reasonably inferred that any height change in the rims of different ages within an individual fossil microatoll should mainly reflect sea-level variation, as the geomorphological and hydrodynamic setting of that specific colony should remain relatively unchanged.

The mid-Holocene samples were taken from precisely recorded positions on the colonies, and their ^{230}Th ages determined to ±0.3–1.0% precision (2 sigma) by thermal ionization mass spectrometry (TIMS) U-series method (see Table 1). The results show that the U-series ages of these microatoll rims range from 7050±32 to 6603±41 yr bp (years before AD 1950) and their elevations vary from 178.5 to 218.5 cm above the modern *Porites* microatoll surfaces. The micro-geomorphology of these microatolls suggests that the elevation differences between these rims mainly resulted from sea-level fluctuations.

The TIMS U-series analytical procedures were those described in Zhao et al. (2001) and Yu et al. (2006). Unaltered coral chips free of any weathered surfaces were extracted from each of the coral specimens, cleaned ultrasonically, and spiked with a ^{229}Th–^{233}U–^{236}U mixed tracer. The ^{233}U–^{236}U double spike with precisely known ^{233}U/^{236}U ratio was used to monitor and correct for U mass-fractionation to improve the analytical precision of U isotope ratio measurements. After total dissolution in nitric acid, concentrated hydrogen peroxide was added to decompose any organic matter and to ensure complete mixing between the spike and the sample. U and Th were co-precipitated with iron hydroxide, and then redissolved

https://doi.org/10.1016/j.yqres.2009.02.003 Published online by Cambridge University Press

Table 1
TIMS U-series isotopic data and elevation measurements (relative to modern living microatolls) for microatoll cores and rims from Leizhou Peninsula, northern coast of the South China Sea.

Microatoll number	Sample name	*U* (ppm)	^{232}Th (ppb)	(^{230}Th/^{232}Th)	(^{230}Th/^{238}U)	(^{234}U/^{238}U)	Uncorr. age (yr)	Corr. age (yr)	yr bp: before AD 1950	Initial (^{234}U/^{238}U)	δ^{234}U(T)	Elevation (cm)	Diameter (cm)
1	FPO-22	2.7668 ± 09	9.914	59.34	0.06921 ± 68	1.1450 ± 09	6850 ± 52	6758 ± 69	6704 ± 69	1.1479 ± 09	147.9 ± 0.9	187.5	54
	FPO-23	2.7837 ± 16	5.874	98.90	0.00069 ± 37	1.1461 ± 14	6711 ± 31	6657 ± 41	6603 ± 41	1.1490 ± 14	149.0 ± 1.4	195.5	130
	FPO-35	2.6287 ± 19	8.871	63.66	0.07074 ± 83	1.1503 ± 15	6889 ± 71	6803 ± 83	6749 ± 83	1.1534 ± 15	153.4 ± 1.5	218.5	93
	FPO-35R1	2.7881 ± 24	8.165	72.72	0.07009 ± 26	1.1437 ± 13	6868 ± 27	6793 ± 46	6739 ± 46	1.1467 ± 13	146.7 ± 1.3		
	FPO-35R2	2.6580 ± 25	4.970	114.2	0.07028 ± 31	1.1457 ± 15	6875 ± 33	6827 ± 41	6773 ± 41	1.1486 ± 15	148.6 ± 1.5		
2	Mean							6810 ± 28	6756 ± 28				
	FPO-36	2.7512 ± 09	1.448	405.10	0.07000 ± 38	1.1449 ± 12	6868 ± 28	6855 ± 29	6801 ± 29	1.1478 ± 13	147.8 ± 1.3	190.5	
	FPO-36R	2.8375 ± 25	1.595	380.3	0.07037 ± 22	1.1454 ± 9	6887 ± 23	6873 ± 24	6819 ± 24	1.1483 ± 9	148.3 ± 0.9		
	Mean							6865 ± 18	6811 ± 18				
	FPO-26	3.1461 ± 16	4.417	152.1	0.07028 ± 51	1.1416 ± 12	6901 ± 52	6864 ± 55	6810 ± 55	1.1445 ± 13	144.5 ± 1.3	196.5	
3	FPO-27	3.0178 ± 17	3.625	175.0	0.06920 ± 20	1.1448 ± 14	6771 ± 18	6740 ± 24	6686 ± 24	1.1477 ± 14	147.7 ± 1.4	185.5	
	FPO-29	2.6683 ± 28	2.088	275.1	0.07079 ± 20	1.1461 ± 17	6928 ± 21	6908 ± 24	6854 ± 24	1.1490 ± 17	149.0 ± 1.7	203.5	960
	FPO-30	2.7607 ± 14	0.741	794.1	0.07018 ± 65	1.1478 ± 15	6852 ± 66	6845 ± 66	6791 ± 66	1.1507 ± 15	150.7 ± 1.5	196.5	
	FPO-31	2.8816 ± 25	7.353	86.6	0.07269 ± 20	1.1443 ± 15	7129 ± 25	7063 ± 41	7009 ± 41	1.1474 ± 15	147.4 ± 1.5	192.5	
4	FPO-37	2.9775 ± 12	2.185	292.8	0.07062 ± 28	1.1407 ± 13	6950 ± 23	6931 ± 25	6877 ± 25	1.1436 ± 13	143.6 ± 1.3	204.5	65
	FPO-38	2.8941 ± 24	11.622	53.49	0.07068 ± 29	1.1453 ± 12	6919 ± 30	6816 ± 60	6762 ± 60	1.1484 ± 12	148.4 ± 12	204.5	116
	FPO-40	2.7871 ± 21	32.848	19.17	0.07436 ± 61	1.1459 ± 16	7287 ± 49	6984 ± 158	6930 ± 158	1.1493 ± 16	149.3 ± 1.6	180.5	450
	FPO-40R1	2.7795 ± 17	9.781	62.24	0.07207 ± 26	1.1465 ± 15	7051 ± 27	6961 ± 53	6907 ± 53	1.1496 ± 12	149.6 ± 1.2		
5	FPO-40R2	2.7498 ± 21	15.642	38.66	0.07237 ± 24	1.1463 ± 16	7082 ± 26	6936 ± 77	6882 ± 77	1.1495 ± 15	149.5 ± 1.5		
	Mean							6955 ± 44	6901 ± 44				
	FPO-41	2.6487 ± 22	4.851	121.0	0.07292 ± 16	1.1444 ± 21	7151 ± 22	7104 ± 32	7050 ± 32	1.1474 ± 22	147.4 ± 2.2	178.5	200

Note. U-series analytical method is similar to those described in Zhao et al. (2001), except that in the new procedure a ^{233}U–^{236}U double spike was used for mass-fractionation correction. Ratios in parentheses are activity ratios calculated from the atomic ratios. Errors are at 2σ level for the least significant digits. The ages are calculated using Isoplot 2.3/EX program [Ludwig, 2000]. "Corr." and "uncorr." denote corrected and uncorrected. The corrected ^{230}Th ages and initial (^{234}U/^{238}U) ratios include a negligible to small correction for initial/detrital U and Th using average crustal ^{232}Th/^{238}U atomic ratio of 3.8 ± 1.9 (^{230}Th, ^{234}U and ^{238}U are assumed to be in secular equilibrium). R refers to repeated measurement.

in nitric acid prior to purification using standard anion-exchange methods. The U and Th fractions were loaded onto individual pre-degassed, zone-refined rhenium filaments and sandwiched between two graphite layers. Th and U isotopic ratios were measured on a Daly ion counter by TIMS at the University of Queensland. The ^{230}Th/^{238}U and ^{234}U/^{238}U activity ratios were calculated using decay constants of Cheng et al. (2000). The U-series ages (Table 1) were calculated using Isoplot/Ex version 2 Program of Ludwig (2000), and included corrections for non-radiogenic ^{230}Th assuming average crustal ^{230}Th/^{232}Th ratio of $4.4 \pm 2.2 \times 10^{-6}$ for the non-radiogenic component. 50% uncertainty in the assumed non-radiogenic ^{230}Th/^{232}Th ratio is propagated to the errors of the corrected ^{230}Th ages. Direct measurements of modern corals of known ages suggest that this assumed non-radiogenic ^{230}Th/^{232}Th ratio of $4.4 \pm 2.2 \times 10^{-6}$ is reliable for corals of continental shelf settings at least along the Western Pacific region (Yu et al., 2006; Shen et al., 2008). Except for FPO-40, non-radiogenic ^{230}Th in other dated samples contribute 7–146 yr (average 56 yr) to the uncorrected ages, and magnified the uncertainties in the corrected ^{230}Th ages by 1–56 yr (average 13 yr). Non-radiogenic ^{230}Th correction in FPO-40 is significantly higher (by 303 yr), magnifying the uncertainty of the corrected ^{230}Th ages by 109 yr. In order to improve age precisions for some samples, replicate analyses were undertaken and the weighted mean age of the replicates has a significantly reduced uncertainty. Our U-Th procedural blanks are also routinely monitored. The ^{238}U and ^{232}Th blanks are both less than 10×10^{-12} g (mainly from graphite), whereas the ^{230}Th blank is $\sim 3.3 \pm 3.3 \times 10^{-17}$ g, which contributes less than 0.2 yr to the calculated ^{230}Th ages of samples such as corals containing 2.5 ppm U when about 1-gram material is used.

Discussion

Our microatoll record from Leizhou Peninsula indicates that relative sea level in the South China Sea in the mid-Holocene (7050–6600 yr bp) was about 1.8–2.2 m higher than present, consistent with the *Goniopora* profile record of the same reef (Yu et al., 2004), as well as with sea-level curves for the western Pacific (Chappell, 1983). The presence of emerged coral reefs of mid-Holocene age in a variety of Pacific sites (far-field region) has been interpreted as the result of the combination between the Early Holocene sea-level rise in response to deglaciation followed by the Late Holocene glacio-hydro-isostatic fall in relative sea level (Mitrovica and Milne, 2002; Lambeck et al., 2002; Lambeck and Chappell, 2001). The mid-Holocene sea-level highstands in the South China Sea has been reported previously (Yu et al, 2004; Zhao and Yu, 2002, 2007). This paper will focus on documenting evidence for century-scale sea-level fluctuations in the mid-Holocene.

Although the annual-scale micro-topography is difficult to identify in some microatolls because of erosion, many other microatolls we have surveyed preserve clear morphological structures reflecting rapid sea-level rises and drops during the formation of the microatolls, such as rim-ridges and grooves (e.g. Figs. 2A–C), and rugged surfaces on their growth discontinuities (Figs. 2C, D). Comparison between the exposed and covered areas of the growth discontinuity surface (Figs. 2D, E) clearly indicates that erosion is insignificant. Overall, the morphological structures (rim-ridges and grooves) of these well-preserved microatolls and their age distribution (Table 1) provide unequivocal evidence for cyclic sea-level fluctuations during the period of the microatoll formation. Although the elevation measurements of some poorly preserved microatolls may not reliably record sea levels, they at least reflect the minimum magnitudes of sea-level fluctuations.

Microatoll-1 (Fig. 3A, 20°14.956'N, 109°54.871'E) has a one-rim morphological structure with a clear low-lying groove between the out rim (FPO-23) and the main body (FPO-22). A strong growth discontinuity can be seen from the fresh-cut section. FPO-22 grew on a branching *Goniopora* coral that developed around 7075 yr bp (Yu et al., 2004). The low-lying gouge between FPO-23 and FPO-22 suggests that after growing to the upper limit (highest level of survival) FPO-22 developed laterally at a slightly lower level and then died and generated the growth discontinuity. FPO-23 developed, about 100 yr later, laterally at first with the lower part of FPO-22 as substrate. It then overgrew the lower part and exceeded the

https://doi.org/10.1016/j.yqres.2009.02.003 Published online by Cambridge University Press

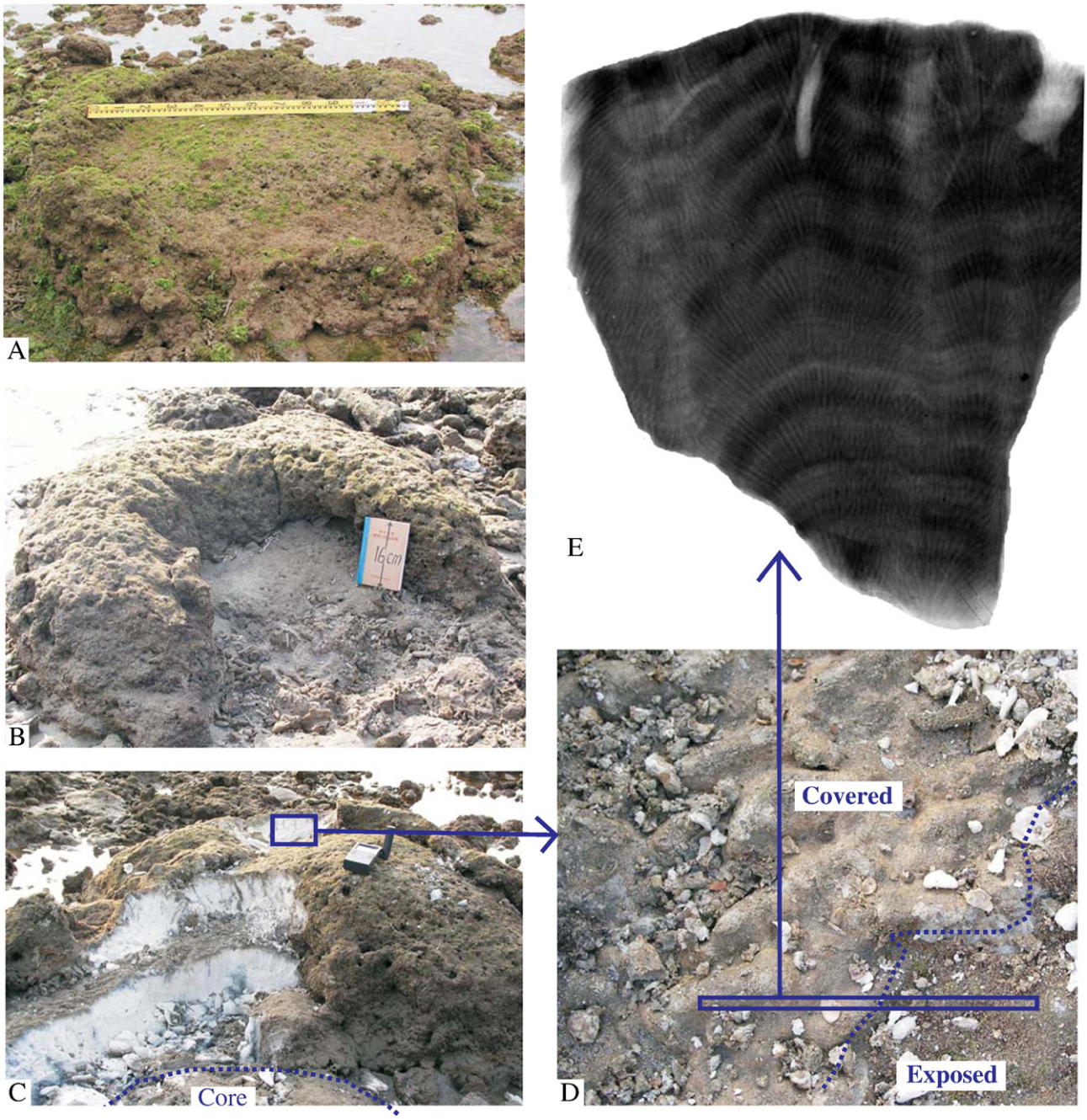

Figure 2. Images of Holocene fossil microatolls on Dengloujiao reef, Leizhou Peninsula, South China Sea, showing macro- and micro-structures and preservation status of these microatolls. Images A and B show microatolls with well-preserved cores and rims. Image C display the open-cuts of the rim of one microatoll. This image clearly shows that the corals are fresh and pristine and growth discontinuities in between different growth phases are well-preserved, reflecting multiple-rim overgrowths as the result of sea-level fluctuations. Image D is an enlarged portion of image C showing the rugged discontinuity surface, with the area to the left of the dotted line being covered by younger rim overgrowth, and the area to the right of the dotted line being exposed. Image E is the X-ray photomicrograph of the cross-section in image D. Note that the erosion in the exposed area (right section) is insignificant if compared with the covered area (left section).

highest point of FPO-22 in elevation. Before wholly covering the main body of FPO-22, FPO-23 stopped vertical growth. From this pattern of growth, we infer a sequence of sea level rising (forming the highest point of FPO-22), stabilizing (lateral development), falling (forming the lower part), and rising again (forming FPO-23). The upper limits of growth of both FPO-22 and FPO-23 may relate to sea level falling, or simply to the colony growing to an upper limit set by duration of subaerial exposure, without change in sea level.

Microatoll-2 (Fig. 3B, 20°14.991'N, 109°54.806'E) is a typical microatoll, consisting of a low-standing core and a high-standing rim, with an outermost diameter of 93 cm. The low-standing core (sample FPO-36) developed at 6811 ± 18 yr bp at an elevation of 190.5 cm, then high-standing outer rim (sample FPO-35) developed by growing upwards in about 55 ± 46 yr (to 6756 ± 28 yr bp) to an elevation of 218.5 cm. Its growth may have stopped before an enclosed upper rim formed. The morphology and age distribution of this microatoll clearly records a period of rapid sea-level rise. The elevation and age differences between the core and the rim correspond to an average ~0.51 cm/yr (0.28 to 3.1 cm/yr range) rate of sea-level rise over a period of 55 ± 46 yr, which is much higher than the rate of 0.19 ± 0.04 cm/yr over the period of 1954–1990 AD based on tide gauge records from Hong Kong, ~480 km away from our site (Ding et al., 2001).

https://doi.org/10.1016/j.yqres.2009.02.003 Published online by Cambridge University Press

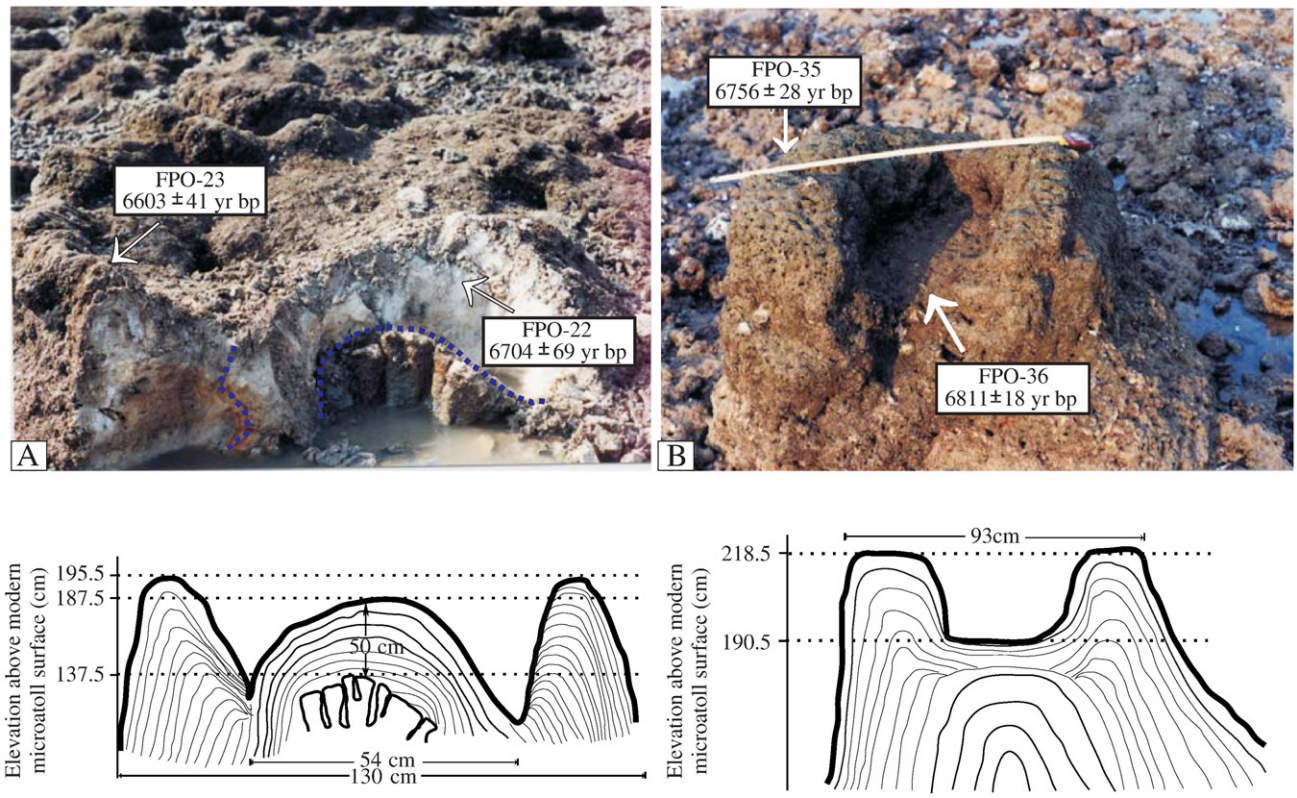

Figure 3. Photographs and rim ages for (A) Microatoll-1 and (B) Microatoll-2. Arrows indicate where samples for U-series dating were collected. The rough development process is schematically illustrated below each microatoll pictures.

Microatoll-3 (Fig. 4A, 20°14.955'N, 109°54.843'E), with a diameter of 960 cm, is a multiple-rim microatoll, with conspicuous low-lying gouges between rims in its geomorphology. The inner-most core (FPO-31) developed about 7009 ± 41 yr bp, and then started the lateral development at a lower level after reaching its highest point. The first rim (FPO-29) developed in 6854 ± 24 yr bp with the lower part of FPO-31 as basement, and also started the lateral development after reaching its highest point. Later, the second rim (FPO-26 and FPO-30) and the third rim (FPO-27) repeated the former process of development respectively in 6791 ± 66 to 6810 ± 55 (with a weighted mean of 6802 ± 42 yr bp) and 6686 ± 24 yr bp, with roughly 100-year cycles. There are some geomorphological breaks in the second rim, so we collected two samples from this rim (FPO-26 and FPO-30). The breaks could have been produced by later weathering process, or by discontinuities in the preexisting coral areas from which the separate sections of Rim-1 grew. Overall, the preservation status of the microatoll is poorer than the others, suggesting that the elevations of the rims only recorded the minimum magnitudes of sea-level fluctuations. In addition, we suspect that one rim between Rim-2 and Rim-3 may have been eroded, probably represented by the highly-elevated remnant to the left of FPO-26 in the photo.

Microatoll-4 (Fig. 4B, 20°14.978'N, 109°54.803'E) has a one-rim structure, with a growth discontinuity between the outer rim (FPO-38) and the inner core (FPO-37). The inner core, with a diameter of 65 cm, developed at about 6877 ± 25 yr bp, then the outer rim, with rim width about 26 cm and a diameter of 116 cm, developed around 6762 ± 60 yr bp on the lateral wall of FPO-37. Both the outer rim and the inner core are in the same elevation.

Microatoll-5 (Fig. 4C, 20°14.962'N, 109°54.794'E) also has a one-rim structure, but with a large low-lying groove between the out rim (FPO-40, diameter 450 cm) and the inner core (FPO-41, diameter 200 cm). Like Microatoll-1, the inner core developed first and then it grew laterally at a lower level at about 7050 ± 32 yr bp. The outer rim grew on the lower part and grew over and above the lower surface at about 6901 ± 44 yr bp, but before covering the whole surface, its growth stopped.

The variations in detailed growths among all the five microatolls, and their differences in height on the reef flat, suggest that on Leizhou Peninsula, multiple sea-level fluctuations were superimposed on the high sea level in the mid-Holocene warm period. If all microatoll rim and core ages are plotted against their elevations (Fig. 5), at least four major cycles of sea-level fluctuations can be identified to have occurred during 7050–6920, 6920–6820, 6820–6690, 6690–? yr bp. Considering the elevation range of the living microatolls and the fact that the microatoll development is mainly controlled by sea levels, the amplitudes of these sea-level fluctuations were about 20–40 cm (overall elevations varying from 178.5 to 218.5 cm above the present sea level), with the highest sea level occurring around 6760 yr bp at about 218.5 cm above the present. During this ~450 yr period, the fastest sea level rising, registered in Microatoll-2, occurred from 6811 (at elevation of 190.5 cm) to 6756 yr bp (at elevation of 218.5 cm) with an amplitude of 28 cm and a rate of ~0.51 cm/yr. Even if the age uncertainties are taken into consideration, the minimum rate of sea-level rise during this period was still about 0.28 cm/yr (or 28 cm/101 yr).

It is worth noting that the above-reconstructed sea-level curve only represents minimum cycles of fluctuation, because the low-lying gouges were not dated. The amplitudes of sea-level fluctuations should also be treated as representing minimum values considering erosion effects on some microatolls. Nevertheless, it is safe to conclude that mid-Holocene sea level has indeed fluctuated on multi-decadal to century scales, a finding that has profound implications for understanding future sea-level trend. This pilot study demonstrates that detailed structural and topographical

https://doi.org/10.1016/j.yqres.2009.02.003 Published online by Cambridge University Press

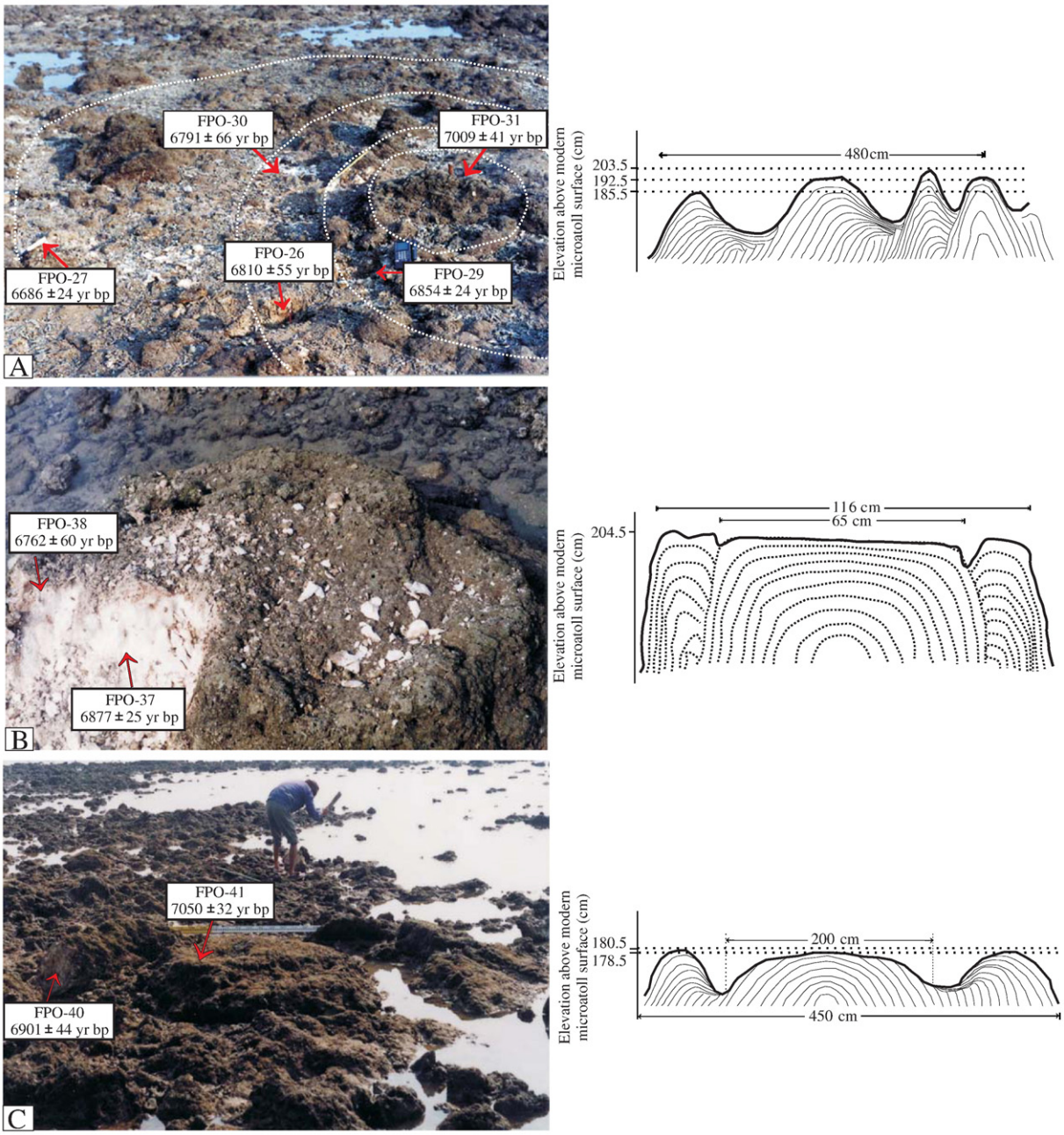

Figure 4. Photographs and rim ages for (A) Microatoll-3, (B) Microatoll-4, and (C) Microatoll-5. Arrows indicate where samples for U-series dating were collected. The rough development process is schematically illustrated at right side of each microatoll picture.

survey of fossil microatolls combined with high-precision dating can provide a promising means for reconstruction of detailed past sea-level excursions.

Conclusions

Our study on the mid-Holocene microatolls indicates that the sea level during the period of 7050–6600 yr bp was about 171 to 219 cm higher than the present, and it showed at least four cycles of fluctuations with amplitudes up to 20–40 cm on century scales. Our study demonstrated that precisely and accurately surveyed and dated reef-flat microatolls have a great potential for the reconstruction of detailed sea-level curve, especially for the past millennium as microatoll samples of these ages are better preserved and can be more precisely dated with an uncertainty of only a few years. In

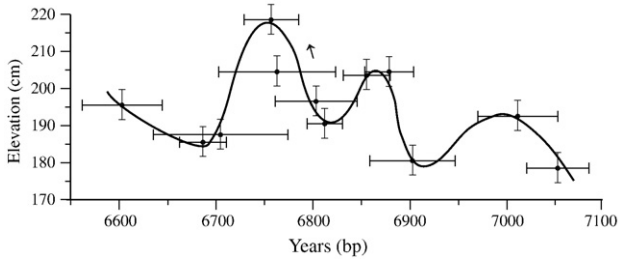

Figure 5. Microatoll-based mid-Holocene sea-level fluctuations. Note that the weighted mean age of 6802 ± 42 yr bp for samples FPO-26 and FPO-30 from Rim-2 of Microatoll-3 (see Table 1) is used for plotting. The elevation range (±8.5 cm) of living microatoll surfaces at the study site is used as a vertical error bar.

https://doi.org/10.1016/j.yqres.2009.02.003 Published online by Cambridge University Press

addition, our results also have implications for the future rates of sea-level change and their impact on coral reefs. A rise of 0.5–0.9 °C (to the SST level of the mid-Holocene as recorded in the study area) is only towards the lower end of IPCC projections (IPCC, 2001) for SST rise during the 21st Century. Thus, it is reasonable to infer similar amplitudes of sea-level fluctuations as recorded in the study area for the near future. If SST rises towards the higher end of IPCC projections (4–6 °C), sea-level fluctuations and combined impact on coral reefs could be catastrophic.

Acknowledgments

This work was funded by the Chinese Academy of Sciences Innovation Program (No. kzcx2-yw-318), the National Natural Science Foundation of China (Nos. 40572102 and 40830852), the Chinese Ministry of Science and Technology projects (Nos. 2006BAB19B03 and 2007CB815905), and ARC projects (DP0773081 and LX0559831). We thank Mike Barbetti and Colin Woodroffe for valuable discussions during the initial drafting of the manuscript, and Alan Gillespie, Claudine Stirling and an anonymous reviewer for constructive comments and suggestions which help the improvement of this manuscript.

References

Chappell, J., 1983. Evidence for smoothly falling sea-level relative to north Queensland, Australia, during the past 6,000 yr. Nature 302 (5907), 406–408.
Cheng, H., Edwards, R.L., Hoff, J., Gallup, C.D., Richards, D.A., Asmerom, Y., 2000. The half-lives of uranium-234 and thorium-230. Chemical Geology 169, 17–33.
Ding, X., Zheng, D., Chen, Y., Chao, J., Li, Z., 2001. Sea level change in Hong Kong from tide gauge measurements of 1954–1999. Journal of Geodesy 74 (10), 683–689.
Flora, C.J., Ely, P.S., 2003. Surface growth rings of *Porites lutea* microatolls accurately track their annual growth. Northwest Science 77 (3), 237–245.
Gagan, M.K., Ayliffe, L.K., Hopley, D., Cali, J.A., Mortimer, G.E., Chappell, J., McCulloch, M.T., Head, M.J., 1998. Temperature and surface-ocean water balance of the mid-Holocene tropical Western Pacific. Science 279 (5353), 1014–1018.
Guilcher, A., 1988. Coral Reef Geomorphology. John Wiley & Sons, Chichester. New York. Brisbane. Toronto. Singapora.
Habrant, N., Lathuiliere, B., 2000. Jurassic corals as emersion indicators. Lethaia 33 (4), 341–344.
IPCC, 2001. Climate Change 2001: Synthesis Report. A Contribution of Working Groups I, II, and III to the Third Assessment Report of the Intergovernmental Panel on Climate Change. Cambridge University Press, Cambridge. 398pp.
Lambeck, K., Chappell, J., 2001. Sea level change through the last glacial cycle. Science 292, 679–686.
Lambeck, K., Esat, T.M., Potter, E.K., 2002. Links between climate and sea levels for the past three million years. Nature 419, 199–206.
Ludwig, K.R., 2000. Users manual for Isoplot/Ex version 2.3 — a geochronological toolkit for Microsoft Excel. Berkeley Geochronology Center Special Publication No. 1a, 54 pp.
Lu, L.Q., 1997. Study on the modern vertical movements along Guangdong coast. Southchina Earthquake 17 (1), 25–33.
McLean, R.F., Stoddart, D.R., Hopley, D., Polach, H., 1978. Sea level change in the Holocene on the northern Great Barrier Reef. Philosophical Transactions of the Royal Society of London Series A 291, 167–186.
Mitrovica, J.X., Milne, G.A., 2002. On the origin of late Holocene sea-level highstands within equatorial ocean basins. Quaternary Science Reviews 21 (20–22), 2179–2190.
Natawidjaja, D.H., Sieh, K., Ward, S.N., Cheng, H., Edwards, R.L., Galetzka, J., Suwargadi, B.W., 2004. Paleogeodetic records of seismic and aseismic subduction from central Sumatran microatolls, Indonesia. J. Geophys. Res.-Solid Earth 109 (B4), doi:10.1029/2003JB002398.
Nie, B.F., Chen, T.G., Liang, M.T., Zhong, J.L., Yu, K.F., 1997. Coral reefs from Leizhou Peninsula and Holocene sea level highstands. Chinese Science Bulletin (in Chinese) 42 (5), 511–514.
Nott, J.F., 2003. The urban geology of Cairns, Queensland, Australia. Quaternary International 103, 75–82.
Nunn, P.D., 2000. Significance of emerged Holocene corals around Ovalau and Moturiki islands, Fiji, southwest Pacific. Marine Geology 163 (1–4), 345–351.
Nunn, P.D., Peltier, W.R., 2001. Far-field test of the ICE-4G model of global isostatic response to deglaciation using empirical and theoretical Holocene sea-level reconstructions for the Fiji Islands, southwestern Pacific. Quaternary Research 55 (2), 203–214.
Scoffin, T.P., Stoddart, D.R., 1978. Nature and significance of micro-atolls. Philosophical Transactions of the Royal Society of London Series B-Biological Sciences 284 (999), 99–122.
Shen, C.C., Li, K.S., Sieh, K., Natawidjaja, D., Cheng, H., Wang, X., Edwards, R.L., Lam, D.D., Hsieh, Y.T., Fan, T.Y., Meltzner, A.J., Taylor, F.W., Quinn, T.M., Chiang, H.W., Kilbourne, K.H., 2008. Variation of initial Th-230/Th-232 and limits of high precision U-Th dating of shallow-water corals. Geochimica Et Cosmochimica Acta 72 (17), 4201–4223.
Smithers, S.G., Woodroffe, C.D., 2000. Microatolls as sea-level indicators on a mid-ocean atoll. Marine Geology 168 (1–4), 61–78.
Smithers, S.G., Woodroffe, C.D., 2001. Coral microatolls and 20th century sea level in the eastern Indian Ocean. Earth and Planetary Science Letters 191 (1–2), 173–184.
Spencer, T., Tudhope, A.W., French, J.R., Scoffin, T.P., Utanga, A., 1997. Reconstructing sealevel change from coral microatolls, Tongareva (Penrhyn) Atoll, northern Cook Islands. 8th International Coral Reef Symposium, pp. 489–494.
Steven, A.D.L., Atkinson, M.J., 2003. Nutrient uptake by coral-reef microatolls. Coral Reefs 22 (2), 197–204.
Stoddart, D.R., Scoffin, T.P., 1979. Microatolls: review of form, origin and terminology. Atoll Research Bulletin 224, 1–17.
Taylor, F.W., Frohlich, C., Lecolle, J., Strecker, M., 1987. Analysis of partially emerged corals and reef terraces in the central Vanuatu Arc — comparison of contemporary coseismic and nonseismic with Quaternary Vertical Movements. Journal of Geophysical Research-Solid Earth and Planets 92 (B6), 4905–4933.
Woodroffe, C., McLean, R., 1990. Microatolls and recent sea-level change on coral atolls. Nature 344 (6266), 531–534.
Woodroffe, C.D., Gagan, M.K., 2000. Coral microatolls from the central Pacific record late Holocene El Nino. Geophysical Research Letters 27 (10), 1511–1514.
Woodroffe, C.D., McLean, R.F., Smithers, S.G., Lawson, E.M., 1999. Atoll reef–island formation and response to sea-level change: West Island, Cocos (Keeling) Islands. Marine Geology 160 (1–2), 85–104.
Yu, K.F., Liu, D.S., Shen, C.D., Zhao, J.X., Chen, T.G., Zhong, J.L., Zhao, H.T., Song, C.J., 2002a. High-frequency climatic oscillations recorded in a Holocene coral reef at Leizhou Peninsula, South China Sea. Science in China Series D-Earth Sciences 45 (12), 1057–1067.
Yu, K.F., Zhao, J.X., Liu, T.S., Wei, G.H., Wang, P.X., Collerson, K.D., 2004. High-frequency winter cooling and reef coral mortality during the Holocene climatic optimum. Earth and Planetary Science Letters 224 (1–2), 143–155.
Yu, K.F., Zhao, J.X., Wei, G.J., Cheng, X.R., Chen, T.G., Felis, T., Wang, P.X., Liu, T.S., 2005. $\delta^{18}O$, Sr/Ca and Mg/Ca records of *Porites lutea* corals from Leizhou Peninsula, northern South China Sea and their applicability as paleothermometers. Palaeogeography Palaeoclimatology Palaeoecology 218 (1–2), 57–73.
Yu, K.F., Zhong, J.L., Zhao, J.X., Shen, C.D., Chen, T.G., Liu, D.S., 2002b. Biological–geomorphological zones in a coral reef area at southwest Leizhou Peninsula unveil multiple sea level high-stands in the Holocene. Marine Geology & Quaternary Geology (in Chinese with English abstract) 22 (2), 27–33.
Yu, K.F., Zhao, J.X., Shi, Q., Collerson, K.D., Wang, P.X., Liu, T.S., 2006. U-series dating of dead *Porites* corals in the South China Sea: evidence for episodic coral mortality over the past two centuries. Quaternary Geochronology 1 (2), 129–141.
Zachariasen, J., Sieh, K., Taylor, F.W., Edwards, R.L., Hantoro, W.S., 1999. Submergence and uplift associated with the giant 1833 Sumatran subduction earthquake: evidence from coral microatolls. Journal of Geophysical Research-Solid Earth 104 (B1), 895–919.
Zachariasen, J., Sieh, K., Taylor, F.W., Hantoro, W.S., 2000. Modem vertical deformation above the Sumatran subduction zone: paleogeodetic insights from coral microatolls. Bulletin of the Seismological Society of America 90 (4), 897–913.
Zhao, J.X., Hu, K., Collerson, K.D., Xu, H.K., 2001. Thermal ionization mass spectrometry U-series dating of a hominid site near Nanjing, China. Geology 29, 27–30.
Zhao, J.X., Yu, K.F., 2002. Timing of Holocene sea-level highstands by mass spectrometric U-series ages of a coral reef from Leizhou Peninsula, South China Sea. Chinese Science Bulletin 47 (4), 348–352.
Zhao, J.X., Yu, K.F., 2007. Millennial-, century- and decadal-scale oscillations of Holocene sea-level recorded in a coral reef in the northern South China Sea. Quaternary International 167–168, 473.
Zhang, Z.K., Meng, H.M., Wang, W.F., Li, Y.M., You, K.Y., Yu, K.F., 2008. Preliminary study on the coastal sediments records about the historical earthquake in the year of 1605 AD, Hainan Island, China. Marine Geology & Quaternary Geology 28 (3), 9–14.